EMI Suppression of 10 Gbit/s Optical Transceiver by Using EBG Structure

Daisuke KAWASE*, Hiroyasu OOMORI, Hiroshi KAWAMURA, Takashi KONDOU, Manabu SHIOZAKI and Hiromi KURASHIMA

The fiber optic data transmission system plays an important role in broadband communication. According to the market trend, data traffic is significantly increasing and larger throughput of communication systems is required. Many electro-optical conversion devices (so called optical transceivers) are used in the system. Because of that, the electro-magnetic noise radiation becomes a serious issue. Although the noise level is proportional to the number of transceivers, a qualitative relationship between the number of transceivers and emission level is not clear. Furthermore, since there's no general design guideline to suppress electro-magnetic interference (EMI), it is difficult to solve this problem once it emerges. In these circumstances, recent dispersion control technology, such as Electro-magnetic Band Gap (EBG), is a potential solution for this problem. In this paper, the methods of how to predict the total emission level with the superimposed effect of hundreds of transceivers and how to determine the EMI suppression design target are described. Then, the method of how to reach the targeted noise level with a newly introduced shielding scheme is explained. Finally, the result of an in-house prototype test is summarized, which proves the verification of the EBG structure by utilizing FEM/FDTD simulation.

Keywords: optical transceiver, EBG

1. Introduction

Optical transceivers are used for high speed fiber optic digital communication. The commercial application has already been implemented in current optical networks. It is often said that "noise free" is one benefit of optical communication systems. However, this is not necessarily true in the case of an electro-optical conversion function block. Since a photon is just the carrier of the signal in the optical fiber, a conversion process from the electrical signal to photonic signal and vice versa is required. During this process of converting electrons to photons, a certain amount of high frequency noise can spread into the space, and it may cause electro-magnetic interference (EMI). State-of-the-art data processing equipment, such as a router, can handle more than 300 Tbit/s data throughput. This equipment may require hundreds of optical transceivers and the noise generated may increase with the number of implemented transceivers. To prevent each transceiver from having an interference problem, it is a requirement to meet the industrial regulation specified by CFR(1) or CISPR(2). As shown in this study, an optical transceiver has a complex relationship regarding EMI issues, and its prevention is the main topic of this paper.

Our major interests are, 1) how much EMI suppression for the individual transceiver is required according to the case of larger systems, and 2) how to suppress EMI emission level from the module with regard to the target determined above. Basically, this paper consists of three parts. First, the EMI emission performance of our current optical transceiver is shown, and the issues are described. Second, the superimposed effect for the radiation is estimated, when a number of transceivers are operated. This trial is basically done by mathematical analysis instead of actual testing. A simple simulation model can be sufficiently demonstrated to predict the effect and determine our design target from the result. And thirdly, a new shielding scheme utilizing Electro-magnetic Band Gap (EBG) technology is introduced, starting from its basic concept and design process. Finally, the evaluation result is demonstrated.

2. EMI Issue of an Optical Transceiver

A typical optical transceiver is indicated in **Fig. 1**. It is an electro-optical data converter with an intelligent controller and data processer. Another prominent feature is the so called "pluggable(3)" package. This form factor makes it possible to easily insert (or extract) the transceivers into an available slot on the system line card.

2-1 Optical transceiver

A typical optical transceiver consists of a packaged semiconductor laser diode and photodetector connected to a printed circuit board assembly (PCBA). On the PCBA, there is a driver circuit for the laser diode, and an amplifier circuit for the received data. **Figure 1** also illustrates the internal structure and relationship of each element. Components are covered by a metal chassis and the optical transceiver is plugged into the host cage system. The chassis and cage system are connected to the frame ground of the system.

In general terms, the key for noise suppression is to guarantee the sufficient contact of those metal surfaces: chassis to the cage and cage to the frame ground.

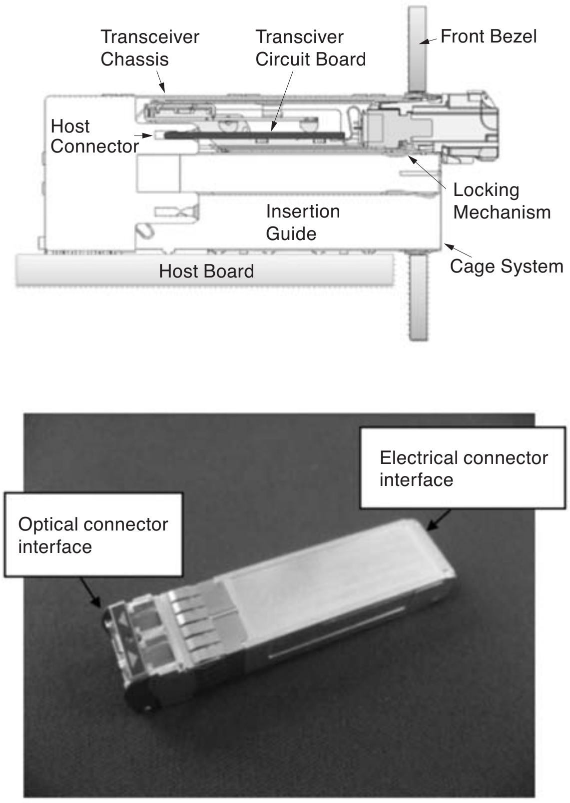

Fig. 1. External view of the optical transceiver "SFP+"

2-2 EMI performance of a single transceiver

The trapezoid waveform is used in the digital data transmission system and it has discrete frequency components. **Table 1** shows the high speed fiber optic applications. This table also shows data rate, clock frequency (fundamental harmonic frequency), and the 2nd and 4th order harmonic frequencies. EMI occurs when the electric circuit in the transceiver operates at a data rate near to 10 Gbit/s.

A consecutive bit sequence is streaming on the actual communication system. Its pattern may have "random" frequency spectrum for a long period of time but that may not be the case for a short period. The worst case should be a consecutive "1010" bit sequence. **Figure 2** shows an experimental result for EMI of a typical Small Factor Pluggable Plus (SFP+) transceiver operating under IEEE802.3ae (so called 10 Gigabit Ethernet[*1]) bit rate and 10 GFC (10 Gbit/s Fiber Channel[*2]) bit rate with a "1010" bit stream. This experiment was conducted according to 47 CFR part 15. Although 60 dBμV/m is specified as the upper limit, 6 dB margin should be considered as a guard band to offset any measurement error. So "less than 54 dBμV/m" is the design target. In **Fig. 2**, H means horizontal polarized wave, and V means vertical polarized wave, respectively. Both polarization modes are imposed in accordance with the regulation. As shown in **Fig. 2**, only the 2nd and 4th order harmonics were observed. This is because of distortion of the waveform, known as duty cycle distortion, by the offset of the cross point.

This result shows that the 21.0375 GHz component has the smallest margin 12 dB below the design target. It is not clear if this margin of the single transceiver measurement would be sufficient in the case of a large system.

As long as the total system has to meet the regulation: less than 54dBμV/m regardless of the number of transceivers, it is quite important to know the relationship between the emission level and the number of transceivers.

Table 1. High speed fiber optic communication standard

	Data rate [Gbit/s]	Fundamental harmonics [GHz]	2nd order harmonics [GHz]	4th order harmonics [GHz]
IEEE802.3ae	10.3125	5.15625	10.3125	20.625
10GFC	10.51875	5.0625	10.51875	21.3125

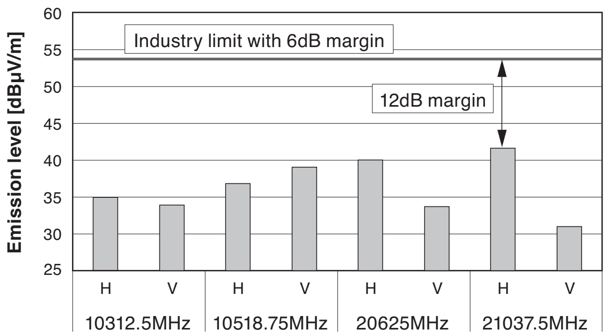

Fig. 2. EMI test result of the individual transceiver

3. Prediction of the Superimposed Noise Emission

The first step is to know the allowable limit of the radiation level of the individual transceiver, especially in the case of a large system which has hundreds of optical transceivers. As the number of transceivers increases, total emission will increase. However, the quantitative assumption of the emission level is not so easy since this phenomenon must be treated as the wave propagation. The installed position of the each transceiver and phase of each signal may be difficult to consider. To estimate the effect of these parameters, all the combinations have to be considered. Therefore, probability is used and this issue should be handled as the expectation in probability logic. This is a classic problem which was first researched in the 18th century by Lord Rayleigh, known as Rayleigh fading[(5)]. In the following section, an effective simulation model is described with some assumptions applied for this calculation. To reduce the complexity of the calculation, a theoretical formula was used[(6)]. Finally, the result with a target is presented: allowable noise radiation level for an individual transceiver.

3-1 Simulation model

The simulation model is shown in **Fig. 3**. This model is called the "3 m method" in the anechoic chamber. In this method, the device under test (DUT) is set on a table that is 1 m above ground. A small dipole array shown in **Fig. 3** is set as the noise source to represent the transceiver array. For the measurement setup, first the table is rotated to search for the highest peak and then the antenna is adjusted up and down to find the peak point and peak level. To simplify this action, the DUT is set 1 m above the ground plane and the observance cylindrical plane is set 3 m away from the DUT to find the peak, instead of the rotary table and antenna swing in the actual measurement.

3-2 Simulation method

Electro-Magnetic full wave simulation, such as FDTD*3 or FEM*4, is a versatile tool for this kind of problem. However, it may require huge resources because of the model size. To facilitate the simulation, the following theoretical formula was used.

$$\mathbf{E}=\frac{e^{-jkR}}{4\pi\varepsilon R}k^2\left[-(\mathbf{p}\times\mathbf{R}_0)\times\mathbf{R}_0+\left(\frac{j}{kR}+\frac{1}{(kR)^2}\right)\{2(\mathbf{p}\cdot\mathbf{R}_0)\mathbf{R}_0+(\mathbf{p}\times\mathbf{R}_0)\times\mathbf{R}_0\}\right]$$

$$\mathbf{H}=\frac{e^{-jkR}}{4\pi\varepsilon R}\frac{k^2}{Z}\left(-1+\frac{j}{kR}\right)\mathbf{p}\times\mathbf{R}_0$$

Where;

- E Electric field vector [V/m]
- H Magnetic field vector [A/m]
- k Wave number [1/m]
- p Dipole moment [V/m]
- R_0 Unit vector from antenna to an observer [m]
- R Distance from antenna to an observer [m]
- ε Dielectric constant [F/m]
- Z Free space impedance [Ω]
- j Imaginary unit

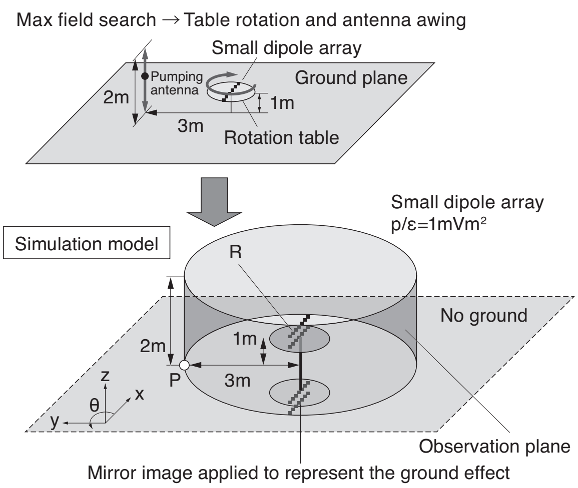

Fig. 3. Simulation model

3-3 Simulation results

This calculation has been carried out with our original FORTRAN*5 program. The applied condition was:

1) 1,000,000 cases of random phase shift combinations.

2) Observance point moved at 5 mm and 0.45 degree pitch. The result is shown in **Fig. 4**. Several cases of the transceiver array, from N = 8 through N = 256, is plotted. The horizontal axis shows the electric field intensity in the arbitrary unit and vertical axis shows the statistical number. The probability distribution of each case looks similar in shape and is nearly a normal distribution. Since the expectation value could be estimated from this result, we calculated the "likelihood" next.

Figure 5 is the tendency of the probable field intensity versus the number of transceivers. In this figure, 99.9% probability is applied. This probability is equivalent to 3.09 sigma in a normal distribution. As the number of transceivers increases, the total intensity also increases but the absolute value of the peak level is not proportional to the number of transceivers. According to our investigation, if the number of transceivers is doubled, the intensity peak is 1.41 times (square root of 2) larger than the previous value. This is almost equivalent to the superposition of a random phase wave. This result is confirmed by the following simple calculation. When the number of noise sources is n, we defined the electromagnetic energy and the maximum intensity of electric field as P_n and E_n. If the number of noise sources becomes 2n, the total electromagnetic energy $P_{2n} = 2P_n$. From the relation of $P_n \propto |E_n|^2$, the equality $|E_{2n}| = 2^{1/2}|E_n|$ is obtained.

The equivalent single emission level can be calculated to meet "total emission level less than 54 dBμV/m." As a

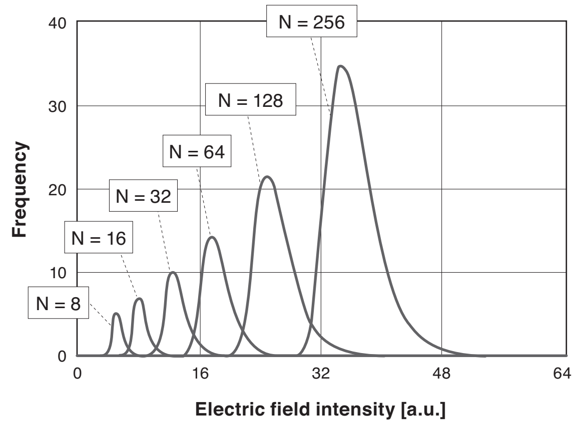

Fig. 4. Simulation result of various array number from N=8 to N=256

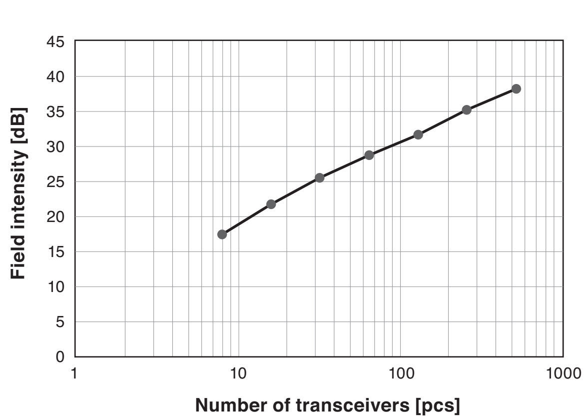

Fig. 5. Relationship of the field intensity and the number of noise source

first step, the case of 100 transceivers was chosen. This means an approximate 30 dB enhancement from the single emission. Therefore, an emission level of 25 dBμV/m was determined as the new target.

Referring back to **Fig. 2**, another suppression scheme is required especially at the 21.0375 GHz range.

4. Novel Shielding for Further EMI Suppression

To meet the requirement, the EMI physics should be understood so as to take the most effective actions for solving the current problem. The use of a microwave absorber is one feasible solution. However, this is not a cost effective solution. Therefore, it was necessary to focus on a new dispersion control scheme, such as the composite right and left handed (CRLH) meta-materials. CRLH is presented as a general transmission line possessing both left-handed (series capacitors and shunt inductors) and right-handed (series inductors and shunt capacitors) structures[7] and the electromagnetic band gap (EBG) which is a region of frequency where the electromagnetic wave cannot propagate[8]. They have been researched and effectively applied for microwave components, such as antennas, filters, and of course, for noise suppression. One benefit is that the scheme can be realized by periodic structures where no special material is required and can be built into the chassis.

This section describes the results with EBG structure. First, issues of the current design are explained. Then, there is one potential solution based on the EBG structure. Secondly, the theoretical background of EBG and the actual structure are described. After some analytical review, an FEM simulation model and simulation result are presented. Lastly, details of an actual sample and experimental result are presented.

4-1 Weak point of the current shielding

To find out the fundamental issue, experiments were carried out in an “ideal” box for emission measurement: a transceiver surrounded by metal to eliminate any cause of radiation from the joint of the chassis and other mechanical parts. This is the best possible measurement box. **Figure 6** shows the schematic of the test setup and **Fig. 7** shows the result.

Through the experiment, the following facts were found.

1) EMI for the 2nd order harmonics range (10.3125 or 10.51875 GHz) is significantly improved by surrounding the chassis with metal. The emission level was below the measurement limit. This situation can be realized by improving the “shielding finger” design.
2) EMI for the 4th order harmonics range (20.625 or 20.375 GHz) is difficult to suppress. No significant change occurred.

Since the transceiver chassis looks like a rectangular tube, it is possible to presume the chassis as a waveguide with 13.8 mm × 8.7 mm cross section. If this estimation is valid, its cut-off frequency is 10.87 GHz. Therefore, theoretically it is conceivable that the 2nd order noise from the transceiver is not expected to propagate but the 4th order can propagate.

Furthermore, since the optical transceiver has an electrical connector and optical connectors, it is difficult to seal the front end area. This may affect the shielding quality for the 4th order harmonics because any small gap more than a few mm could be detrimental to performance at frequencies more than 20 GHz. For this reason, the 4th order harmonics should be decayed inside of the chassis to suppress the total noise emission. To realize this, an EBG periodic structure is employed instead of applying a more costly microwave absorber.

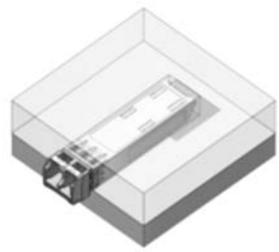

Fig. 6. Transceiver surrounded by metal

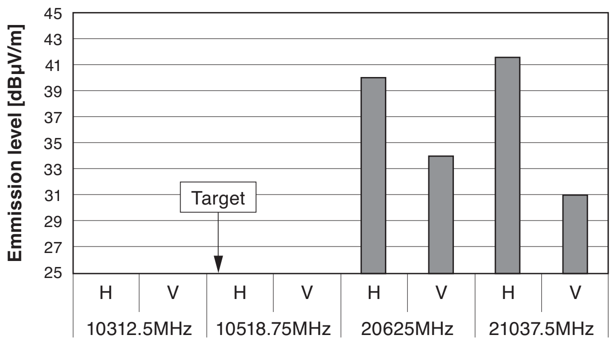

Fig. 7. EMI Result of the possible best shielding

4-2 Background of EBG

A two dimensional EBG was invented in the 1990’s[9]. Its basic concept was found in the 1950’s[10],[11], in waveguide applications. Because of the similarity of the optical transceiver and waveguide, the waveguide technology can be well suited for the optical transceiver’s EMI suppression at specified frequencies. Referring to (12), a diaphragm in the middle of a waveguide composes the transmission line which can be expressed as a circuit consisting of shunt inductors and series capacitors, the so called left handed transmission line. It may be possible to generate a stop band if a periodic structure of these diaphragms is successfully designed according to Floquet’s theorem[13]. However, there are so many unknown parasitic elements, such as conductors, dielectric substance and inductance close to the EBG periodic structure. Therefore, this structure was designed by FDTD analysis.

The EBG structure and evaluation model are shown in **Fig. 8**. Eight diaphragms are set up in the waveguide. Here, the depth of diaphragms is an important parameter.

The depth should be one-quarter wavelength of the target frequency, about 20 GHz(9). When the frequency of the incident wave target is 20 GHz, the top surface becomes a high impedance surface, and the incident wave is reflected by mode mismatch in the waveguide. The reflection characteristic depends on the number of diaphragms. The more the diaphragms increase, the more propagation decreases exponentially. The space between each diaphragm should be sufficiently smaller than the target wavelength(9). For these reasons, the size of the diaphragm was determined to be 12 mm × 3.9 mm × 0.6 mm with a spacing of 0.6 mm. These pitch and thickness values were determined based on manufacturability with Zinc die casting. A small dipole, as a noise source, is put into the wave guide on the left side 24.6 mm apart from the EBG. The transmitted wave was measured at "observer" position.

Figure 9 shows the field potential ratio at an observation point defined in **Fig. 8**. The horizontal axis is frequency and the vertical axis is a power ratio which is defined as voltage at the observer position over the output voltage from the dipole. This result shows the energy component of 21 GHz to 24 GHz is decayed when transmitted to the observer. Therefore, there is a possibility of the existence of the stop band at this frequency range. As mentioned in the previous sections, our target suppression frequency is more than 20.625 GHz. Although the stop band was slightly different from the target frequency, it gave us good foresight into the prospects for improvement. Therefore, more detailed simulations were conducted by FEM analysis.

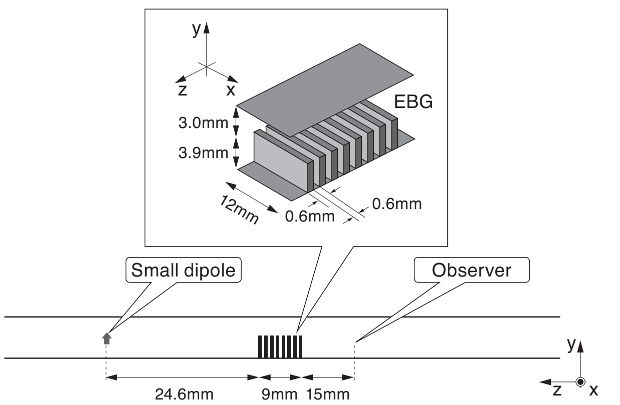

Fig. 8. Simulation model for EBG

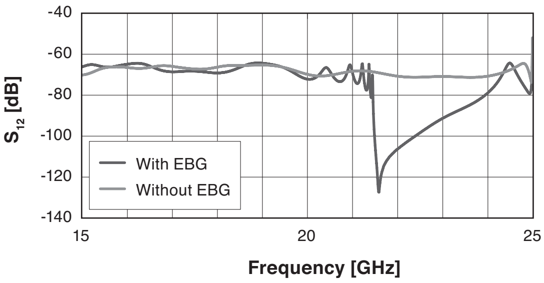

Fig. 9. Scattering parameter result of FDTD simulation

4-3 Simulation Model and Result

The model has the chassis (top and bottom), host connector, electro-optical sub-assembly, PCBA, surface mount devices, optical connector, and external chassis (extreme box). Those dimensions were imported from the CAD*6 system. **Figure 10** shows the result of the electric field distribution at 20.3125 GHz with and without the corrugated structures. Compared to **Fig. 9** in the previous chapter, significant noise reduction effect was observed. The electric field is trapped inside the EBG and there is less electromagnetic noise/field than that without the EBG scheme.

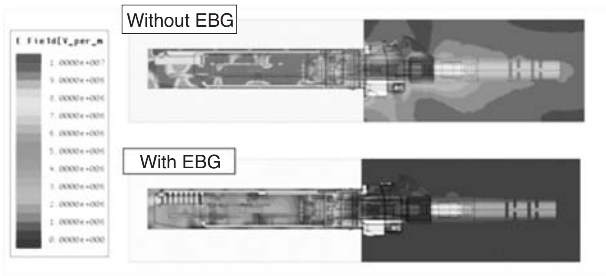

Fig. 10. Field distribution result of the transceiver with EBG. Above; without the EBG structure, below; with EBG structure. Red area indicates the field intensity is high. Although this result includes both near and far field, with corrugated structure shows the field distribution is "calm and quiet."

4-4 Experiment results

Photo 1 shows the photograph of an actual sample. The EMI test was conducted with all the electro-optical components built into that chassis.

Figure 11 summarizes the peak emission values. Frequency ranges are per IEEE803.2ae and 10 GFC. Significant improvement is observed especially at 20.3125 GHz and 21.0375 GHz of horizontal polarization. Although the ultimate goal of 25 dBμV/m was not yet reached, additional improvement is being pursued to achieve it. Next, the reason why only the horizontal polarization shows good suppression will be investigated with the expectation that this will lead to further improvement.

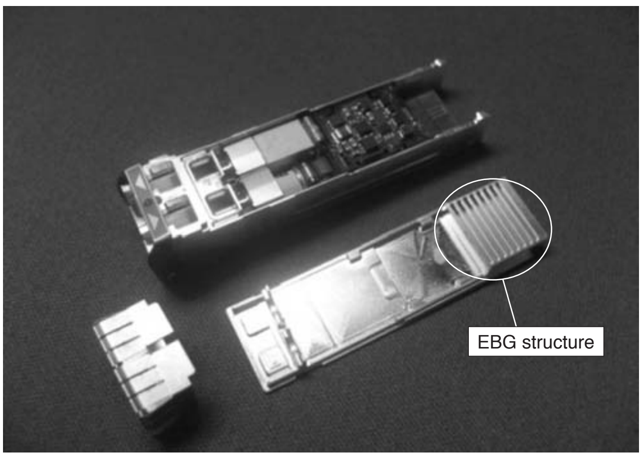

Photo 1. Photograph of the transceiver prototype with corrugated EBG chassis

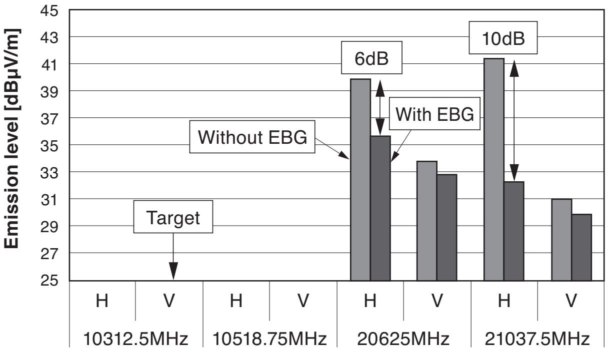

Fig. 11. Comparison of the emission level at the various frequencies

5. Conclusion

A new EMI suppression scheme has been demonstrated. First, the suppression target of an individual transceiver was estimated by calculating superimposed noise emission. Second, the EBG structure on the transceiver chassis was designed utilizing FDTD/FEM simulation and its effectiveness was confirmed by a prototype test.

The EMI suppression issue will become more important as port densities continue to increase. Technologies described in this paper promise the improvement of EMI with EBG as a new scheme for better performance.

Technical Term

*1 10 Gigabit Ethernet: One of the communication standards connecting the computer system to another.
*2 10 Gbit/s Fiber Channel: One of the Gbit/s network technologies.
*3 FDTD: Finite-Difference Time-Domain method. One of the electromagnetic analysis methods.
*4 FEM: Finite Element Method. One of the numerical analysis methods.
*5 FORTRAN: One of the programming languages.
*6 CAD: Computer Aided Design. Design using a computer.

References

(1) Code of Federal Regulation, Title 47 Part 15 Telecommuncation Federal Communication Commission
(2) CISPR 22 Information Technology Equipment – Radio Disturbance Characteristics – Limits and Methods of Measurement.
(3) SFF-8472 Small Form Factor Pluggable MultiSource Agreement.
(4) M. Nishie, "Research and Development of optical datalink," SEI technical review, vol.70, April 2010, p.4.
(5) Sir Lord Rayleigh, "On the resultant of large number of vibrations of the same pitch and of arbitrary phase," Philosophical magazine and journal of science, Aug. 1880, p.71.
(6) H. Hertz: Electric waves, p.144, Dover pub inc.
(7) C. Caloz and T. Itoh, "Novel microwave devices and structures based on the transmission line approach of meta-materials," in IEEE-MTT Int. Symp. Dig., pp.195-198, June 2003.
(8) R. Abhari and G.v. Eleftheriades, "Metallo-dielectric electromagnetic bandgap structures for suppression and isolation of the parallelplate noise in high-speed circuit," IEEE Trans. Microw. Theory Tech., vol.Sl, no.6, pp.1629-1639, June 2003.
(9) D. Sievenpiper, "High-impedance electromagnetic surfaces," Ph.D. dissertation, UCLA electrical engineering department, filed January 1999.
(10) W. Rotman, "A Study of Single-Surface Corrugated Guides," Proc. IRE 39, 952, 1951.
(11) R. Elliot, "On the Theory of Corrugated Plane Surfaces," IRE Trans. Ant. Prop. 2, 71, 1954.
(12) Nathan Marcuvitz, Waveguide Handbook (IEEE Electromagnetic Waves Series), The Institution of Engineering and Technology; First Thus edition, April 1986.
(13) C. Caroz and T. Itoh, "Electromagnetic Metamaterials-Transmission Line theory and Microwave Applications," Wiley-Interscience, A John Wiley & Sons, Inc., Publication, 2006.

Contributors (The lead author is indicated by an asterisk (*).)

D. KAWASE*

• Ph.D. degree in engineering
Transmission Devices R&D Laboratories
He has been engaged in development of optical transceivers.

H. OOMORI
• Assistant manager, Transmission Devices R&D Laboratories

H. KAWAMURA
• Transmission Devices R&D Laboratories

T. KONDOU
• Transmission Devices R&D Laboratories

M. SHIOZAKI
• Assistant General Manager, Transmission Devices R&D Laboratories

H. KURASHIMA
• Senior Assistant Manager, Transmission Devices R&D Laboratories